



**HAL**  
open science

## **Influence of the environmental relative humidity on the inflammatory response of skin model after exposure to various environmental pollutants**

Emeline Seurat, Anthony Verdin, Fabrice Cazier, Dominique Courcot, Richard Fitoussi, Katell Vié, Valérie Desauziers, Isabelle Momas, Nathalie Seta, Sophie Achard

### ► To cite this version:

Emeline Seurat, Anthony Verdin, Fabrice Cazier, Dominique Courcot, Richard Fitoussi, et al.. Influence of the environmental relative humidity on the inflammatory response of skin model after exposure to various environmental pollutants. *Environmental Research*, 2021, 196, pp.110350. 10.1016/j.envres.2020.110350 . hal-03000568

**HAL Id: hal-03000568**

**<https://imt-mines-ales.hal.science/hal-03000568>**

Submitted on 9 May 2023

**HAL** is a multi-disciplinary open access archive for the deposit and dissemination of scientific research documents, whether they are published or not. The documents may come from teaching and research institutions in France or abroad, or from public or private research centers.

L'archive ouverte pluridisciplinaire **HAL**, est destinée au dépôt et à la diffusion de documents scientifiques de niveau recherche, publiés ou non, émanant des établissements d'enseignement et de recherche français ou étrangers, des laboratoires publics ou privés.



Distributed under a Creative Commons Attribution - NonCommercial 4.0 International License

1 **Influence of the environmental relative humidity on the inflammatory**  
2 **response of skin model after exposure to various environmental**  
3 **pollutants**

4

5 Emeline Seurat<sup>a</sup>, Anthony Verdin<sup>b</sup>, Fabrice Cazier<sup>c</sup>, Dominique Courcot<sup>b</sup>, Richard  
6 Fitoussi<sup>d</sup>, Katell Viéd<sup>d</sup>, Valérie Desauziers<sup>e</sup>, Isabelle Momas<sup>a</sup>, Nathalie Seta<sup>a</sup>, Sophie  
7 Achard<sup>a\*</sup>

8

9 <sup>a</sup> Laboratoire de Santé Publique et Environnement, Hera “Health Environmental Risk  
10 Assessment”, Inserm UMR1153-CRESS (Centre de Recherche en Epidémiologie et  
11 StatistiqueS), Université de Paris, Faculté de Pharmacie de Paris, 4, Avenue de  
12 l'Observatoire, 75006 Paris, France

13 <sup>b</sup> Unité de Chimie Environnementale et Interactions sur le Vivant UR4492, SFR  
14 Condorcet FR CNRS 3417, Maison de la Recherche en Environnement Industriel 2,  
15 Université du Littoral Côte d’Opale, 189A Avenue Maurice Schumann, 59140  
16 Dunkerque, France

17 <sup>c</sup> Centre Commun de Mesures (CCM), Université du Littoral-Côte d’Opale, 145  
18 Avenue Maurice Schumann, 5914 Dunkerque, France

19 <sup>d</sup> Laboratoires Clarins, 5 Rue Ampère, 95300 Pontoise, France

20 <sup>e</sup> IPREM, IMT Mines Ales, Université de Pau et des Pays de l’Adour, E2S UPPA,  
21 CNRS, Pau, France

22

23 \*Corresponding author – E-mail address: [sophie.achard@u-paris.fr](mailto:sophie.achard@u-paris.fr)

24 **Abstract**

25 The skin is an essential barrier, protecting the body against the environment and its  
26 numerous pollutants. Several environmental pollutants are known to affect the skin,  
27 inducing premature aging through mechanisms including oxidative stress,  
28 inflammation, and impairment of skin functions. Even climate conditions can impact the  
29 skin. Therefore, using a Reconstructed Human Epidermis (RHE), we tested the effect of  
30 two samples of fine particulate matters (PM<sub>0.3-2.5</sub> – one metals-rich sample and the other  
31 organic compounds-rich), two Volatile Organic Compounds mixtures (VOCs – from a  
32 solvent-based paint and a water-based paint) and Tobacco Smoke (TS). All pollutants  
33 affected cellular functionality, but to a lesser extent for the water-based paint VOC. This  
34 effect was enhanced when RHE were preconditioned for two hours by a semi-dry  
35 airflow (45% relative humidity) before pollutants application, compared to  
36 preconditioning by a humid airflow (90% relative humidity). In the absence of  
37 preconditioning, IL-1 $\alpha$ , IL-6, IL-8, and RANTES were almost systematically induced  
38 by pollutants. When RHE were preconditioned by a semi-dry or humid airflow before  
39 being subjected to pollutants, the increase of IL-1 $\alpha$ , IL-8, and RANTES falls into two  
40 groups. Similarly to RHE not treated with pollutants, RHE treated with VOCs after  
41 preconditioning by a semi-dry airflow showed increased IL-1 $\alpha$ , IL-8, and RANTES  
42 release. On the contrary, RHE treated with PM or TS after preconditioning by a semi-  
43 dry airflow show a lower increase in IL-1 $\alpha$ , IL-8, and RANTES compared to  
44 preconditioning by a humid airflow. The effect of real environmental relative humidity  
45 conditions of the air, combined with acute exposure to various environmental pollutants,  
46 seemed to relate mainly to structural changes of the skin, determining the outcome of

47 the inflammatory response depending on the physicochemical characteristics of  
48 pollutants.

49 **Keywords**

50 3D-Skin model

51 Air Liquid exposure

52 Environmental pollutants

53 Environmental humidity

54 Inflammatory response

55

56 **Abbreviations**

57 DMSO: dimethyl sulfoxide, IL: Interleukin, MMPs: matrix metalloproteinases, MTT: 3-

58 (4,5-dimethylthiazol-2-yl)-2,5-diphenylte-trazolium bromide, PM: particulate matter,

59 RH: relative humidity, RHE: Reconstructed Human Epidermis, ROS: reactive oxygen

60 species, SDS: sodium dodecyl sulfate, TS: tobacco smoke, VOCs: volatile organic

61 compounds.

## 62 **1. Introduction**

63 Air pollution – the degradation of air quality due to harmful gases, chemicals, biological  
64 contaminants, and/or particles – is associated with a variety of acute and chronic  
65 illnesses leading to increased morbidity and mortality (Hoek et al., 2013; Willers et al.,  
66 2013). Like the airway epithelium, the skin is constantly exposed to the environment  
67 and its pollutants. It is essential in protecting the body and many factors can affect it.

68 An obvious intrinsic factor that affects the skin is aging. It is visually characterized by  
69 the appearance of wrinkles, thinner epidermis, cutaneous dryness, ptosis, loss of  
70 elasticity, dark spots, and uneven pigmentation. Central to the process are the increase  
71 of oxidative stress, the increase in the activity of matrix metalloproteinases (MMPs)  
72 leading to degradation of the extracellular matrix, and the increase in the expression of  
73 cytokines and interleukins (Haydont et al., 2019; Parrado et al., 2019). If intrinsic  
74 factors can accelerate these processes, extrinsic factors are also important  
75 (Makrantonaki et al., 2015). The effect of UVs is well known (Jackson et al., 2001;  
76 Flament et al., 2013). Airborne pollutants also exert negative effects on the skin,  
77 especially on sensitive skin that can overreact to external aggression (Krutmann et al.,  
78 2014).

79 For several years, works agreed that Tobacco Smoke (TS) has a strong impact on the  
80 skin. TS is a complex mixture of over 4,000 compounds (CO, HCN, benzene,  
81 formaldehyde, nicotine, phenol, polycyclic aromatic hydrocarbons, *etc.*) and only the  
82 particulate phase, which represents approximately 5% of the cigarette's total output, is  
83 visible as smoke (Hoffmann et al., 1997; Löfrth, 1989; Auer et al., 2017). This complex  
84 mixture leads to premature skin aging, wrinkling, poor wound healing, squamous cell  
85 carcinoma, and chronic dermatoses (Ortiz and Grando, 2012). *In vivo* studies revealed

86 that TS induces reactive oxygen species (ROS), affects collagen production, and  
87 increases the production of tropoelastin as well as MMPs, leading to the degradation of  
88 the extracellular matrix (Morita, 2007). We previously corroborate these results, using  
89 Reconstructed Human Epidermis (RHE), showing that, if two TS exposures are  
90 sufficient to alter the *stratum corneum*, a single one is enough to induce inflammatory  
91 cytokines, MMPs, and oxidative stress, as well as down-regulation of essential skin  
92 functions (Lecas et al., 2016).

93 Outdoor air pollution is made up of gases (O<sub>3</sub>, CO<sub>2</sub>, CO, SO<sub>2</sub>, and NO<sub>x</sub>) and particulate  
94 matters (PM). It is considered the world's largest environmental health risk factor due to  
95 fine (PM<sub>2.5</sub>) and ultrafine (PM<sub>0.1</sub>) particles (WHO, 2018; Loomis et al., 2014). In  
96 addition to the respiratory diseases and premature death they induce (Beelen et al.,  
97 2014; Raaschou-Nielsen et al., 2013), PM are responsible for premature skin aging,  
98 appearance of pigmentation spots, decrease in squalene (a major lipidic component of  
99 sebum) and vitamin E, as well as of the increase of lactic acid and melanin, these later  
100 indicating oxidative stress (Schikowski and Hüls, 2020). Using RHE we showed that  
101 exposure to PM<sub>0.3-2.5</sub> affects cellular functionality, induces the release of inflammatory  
102 cytokines, and leads to oxidative stress (Verdin et al., 2019). PM also have a negative  
103 impact on fundamental skin functions: anchorage, cell differentiation, cornification/skin  
104 desquamation, and apoptosis.

105 Another source of pollution under scrutiny are Volatile Organic Compounds (VOCs).  
106 Defined as organic compounds with a high vapor pressure at normal room temperature  
107 (EU, 2010), they represent a numerous, varied, and ubiquitous group of substances.  
108 Because of the time people spend inside, VOCs emanating from indoor air pollution are  
109 of particular concern. Their sources are numerous including building material,

110 equipment, cleaning products, or even combustion processes such as cooking  
111 (Kostiainen, 1995; WHO, 2010). Some of them (toluene, benzene, ethylbenzene, and  
112 xylene for instance) are known to have serious adverse effects on human health. So far,  
113 the effects of VOCs on the skin is poorly studied. Still, using keratinocytes, Dezest et al.  
114 (2017) suggested that VOCs would play a role in premature skin aging. Indeed, they  
115 show that VOCs inhibit the proteasome, inducing apoptosis, DNA damage, and protein  
116 oxidation.

117 Oxidative stress, inflammation, and metabolic impairments seem to be common  
118 mechanisms of skin aging and pollution-induced premature skin aging. Even climate  
119 conditions – relative humidity, temperatures – impact skin properties and barrier  
120 function and may modify skin reactions (Singh and Maibach, 2013; Cau et al., 2017).

121 Therefore, we evaluated the effect of several pollutants using an RHE system, focusing  
122 on inflammation markers. The pollutants tested are two  $PM_{0.3-2.5}$  samples with different  
123 characteristics, VOCs samples from two different paints and TS. We especially focused  
124 on how semi-dry/humid conditions can affect the inflammation response induced by  
125 pollutants.



## 126 **2. Materials and Methods**

### 127 **2.1. *In vitro* skin model**

128 The *in vitro* skin model used is a reconstructed human epidermis system (RHE) from  
129 SkinEthic™ (Lyon, France; Rosdy and Clauss, 1990; Rosdy et al., 1993). It provides a  
130 differentiated 3D epidermal tissue from human keratinocytes for which signed informed  
131 consent and ethical approval were obtained by the supplier. All experiments were  
132 conducted on a single batch (MF22-5).

133 Culture media, growth medium for non-experiment days, and maintenance medium for  
134 experiment days were supplemented with 1% of Penicillin-Streptomycin mixture  
135 (penicillin: 100 µg/mL; streptomycin: 100UI/mL). Upon reception, RHEs were placed  
136 in a 24-well plate with growth medium on the basal side and maintained in an incubator  
137 at 37 °C, 5% CO<sub>2</sub>, and 95% relative humidity. Experiments were carried out 24h after  
138 RHE-acclimation.

### 139 **2.2. *Fine particulate matters (PM<sub>0.3-2.5</sub>)***

140 Two samples of fine PM, having the same aerodynamic diameter (0.3 to 2.5µm,  
141 PM<sub>0.3-2.5</sub>) and similar granulometric profile, but differing in their sampling origin and  
142 their chemical composition were tested: PM from Cotonou (Benin, West Africa) that are  
143 rich in metals and inorganic elements (PM<sub>m</sub> – metal-rich PM), and PM from  
144 Dunkerque (France) that are rich in organic compounds (PM<sub>o</sub> – organic-rich PM). The  
145 collection and characterization of both PM were already published (Cachon et al., 2014,  
146 Dergham et al., 2015). A summary of their composition is presented in Table 1 and  
147 detailed analysis in Table S1.

148 Aliquoted and kept at -20°C after collection, PM were thawed and suspended in the  
149 maintenance culture medium containing 1% of Penicillin-Streptomycin and 1%

150 fungizone (Thermo Fisher Scientific, Waltham, MA, USA). Twenty-four hours before  
151 experiments, PM suspension was sonicated (50W, 10 min, Bath sonicator Branson  
152 CPXH, Dutscher, France) and 30  $\mu\text{L}$  were deposited onto the apical side of RHEs.  
153 Three concentrations – 3, 15, and 30  $\mu\text{g}/\text{cm}^2$  – as previously described (Verdin et al.,  
154 2019) were tested. Medium without PM was used as a negative control.

### 155 **2.3. Volatile organic compounds (VOCs)**

156 VOC atmospheres were generated from two different paints, which containers have  
157 never been opened). VOCwb (water-based) are from an aqueous paint (Brillant Intérieur  
158 Acrylique, Auchan, France) bought in 2014, after the French regulation governing  
159 construction and decoration labeling (decrees 19/04/2011 and 20/04/2012 that set the  
160 upper limit of VOCs to 20 g/L; European Union, 2010 and the French decree 2011-321  
161 (March 23, 2011) related to the mandatory labeling of VOCs emission of building and  
162 decoration products. VOCsb (solvent-based) are from an alkyd paint (Brillant, Orion  
163 line, Guittet, France) manufactured before 2007, and thus before the above-mentioned  
164 decrees.

165 The protocol applied to generate VOCs atmospheres was inspired by the emission  
166 standard test (ISO 16000-9, ISO, 2006a) and the paints were prepared according to  
167 ISO 16000-11 (ISO, 2006b). Briefly, paint was spread onto a 150  $\text{cm}^2$  glass plate that  
168 was then placed in an 11 L sealed generation chamber under a steady airflow (20-25°C,  
169  $79 \pm 8\%$  humidity and a rate of 0.5 L/h (Ricquebourg et al., 2015). The VOCs  
170 atmosphere was stabilized for 3 days before exposure. Samplings of VOCs from paint  
171 were chemically controlled by vacuum vial SPME sampling (Desauziers and Auguin,  
172 2012) followed by GC/MS/FID analysis. The concentrations of VOCwb and VOCsb

173 were determined as toluene equivalent from the FID signal (Badji et al., 2018) and are  
174 summarized in Table 2 and detailed in Table S2.

175 On the day of exposure, the generation chamber was connected to the Vitrocell®  
176 dynamic exposure system (Vitrocell System® GmbH, Waldkirch, Germany). This  
177 system contains six exposure chambers, each one with an insert with the RHE tissue  
178 and a trumpet. For one hour, a 2mL/min airflow was created to deliver the VOC  
179 atmosphere through the trumpet, onto the apical side of the RHE that was maintained at  
180 37°C thanks to a water bath (Persoz et al., 2010). An atmosphere without VOCs,  
181 delivered with the same dynamic system, was used as a negative control.

#### 182 **2.4. Tobacco smoke (TS)**

183 TS that is a complex mixture containing polycyclic aromatic hydrocarbons, volatile  
184 organic compounds, and PM present in air pollution was used as positive environmental  
185 pollution control. For this purpose, mainstream tobacco smoke (TS) was generated by  
186 the combustion of a French brand cigarette composed of 87% tobacco, 6.5% flavors  
187 agents, and 6.5% cigarette paper. It produces 7 mg of tar, 0.6 mg of nicotine, 9 mg of  
188 carbon monoxide and comprises two parts, gas and particulate matter.

189 Using a static system adapted from the Vitrocell Cloud™ chamber (Vitrocell System®  
190 GmbH, Germany), fresh TS was delivered to the apical face of RHE at a rate of 25 mL  
191 per puff with a total of 10 puffs (Lecas et al., 2016; Bardet et al. 2016). The dose  
192 delivered corresponds to one cigarette, with an average of 200 µg/cm<sup>2</sup> of particulate  
193 matters. Similarly to RHEs treated with VOCs, the air atmosphere used to generate TS  
194 was used as a negative control.

#### 195 **2.5. Exposure of RHEs to pollutants**

196 To compare the effect of the sole pollutants, RHEs were exposed to pollutants as  
197 described above, then incubated for 24h in classical culture conditions (incubator at  
198 37°C, with 5% CO<sub>2</sub>, and 90% relative humidity). RHEs not subjected to pollutant were  
199 used as negative controls (Fig. 1A, 1C).

200 For all experimental series, at the end of the incubation period, culture media were  
201 collected to assess the immune response by quantifying cytokines/chemokines release,  
202 and RHEs were harvested to perform MTT assay.

### 203 ***2.6. Preconditioning of RHE to semi-dry/humid airflow followed by exposure to*** 204 ***pollutants***

205 To assess the role of humidity on the impact of pollutants, RHE were preconditioned by  
206 a semi-dry or humid airflow for 2h before being incubated with pollutants. RHE  
207 maintained at 37°C thanks to a water bath, were subjected to different airflows. The  
208 airflow was delivered using the Vitrocell<sup>®</sup> Humidification Station (Vitrocell Systems<sup>®</sup>  
209 GmbH, Waldkirch, Germany) that was supplying semi-dry air (24°C, 5% CO<sub>2</sub> and 45%  
210 relative humidity (RH) similarly to European conditions like in Dunkerque city) or  
211 humid air (24°C, 5% CO<sub>2</sub> and 90% RH representative of conditions in South America,  
212 Asia or Africa, like in Cotonou city). Then, RHEs were exposed to pollutants as  
213 described above, and further incubated for 24 h in classical culture conditions (37°C,  
214 with 5% CO<sub>2</sub>, and 95% RH) before performing MTT assays on RHE and quantifying  
215 cytokines/chemokines released in the culture media.

216 The protocol of exposure is described in Fig. 1B. Various controls were considered and  
217 are summarized in Fig. 1C. Negative controls: RHEs preconditioned by the humid or  
218 semi-dry airflow but not exposed to pollutants, and RH controls: RHEs exposed to the

219 pollutants but not to preconditioning by the humid/semi-dry airflow (kept in the  
220 incubator at 37°C with 90% RH).

### 221 **2.7. Cellular functionality: MTT assay**

222 Cellular functionality was assayed on the basal side of RHE relying on the ability of the  
223 mitochondrial succinate dehydrogenase to convert MTT (3-(4,5-dimethylthiazol-2-yl)-  
224 2,5-diphenyltetrazolium bromide) into a formazan product that has a maximum  
225 photometric absorbance at 490 nm (Persoz et al., 2010). Briefly, 24h after exposure, the  
226 culture medium was removed, 500 µL of MTT was added to the bottom of the well  
227 containing the RHE. After two hours of incubation (37°C, with 5% CO<sub>2</sub>, and 95%  
228 relative humidity), DMSO (500µL) was added to the bottom of the well, reagents were  
229 homogenized by shaking and transferred to 96-well plates. Absorbance was read using a  
230 microtiter plate reader (Multiskan<sup>®</sup> EX, Thermo Scientific, Waltham, MA, USA).

### 231 **2.8. Mapping of cytokine production: Q-Plex<sup>™</sup> analysis**

232 Q-Plex<sup>™</sup> quantitative ELISA-based chemiluminescent assay (Quansys, Logan, UT,  
233 USA) were performed according to the manufacturer's instructions, using the profiling  
234 service of Tebu-bio (Le Perray-en-Yvelines, France). Nine cytokines (Q-Plex Human  
235 Cytokine-Inflammation #110433HU – IL-1α, IL-1β, IL-2, IL-4, IL-6, IL-8, IL-10,  
236 IFNγ and TNFα) and eight chemokines (Q-Plex Human Chemokine Inflammation  
237 #110451HU – Eotaxin, GROα, I-309, IP-10, MCP-1, MCP-2, RANTES and TARC)  
238 were measured. The analysis was performed by quantifying the intensity of the  
239 chemiluminescent signals on the Tebu-bio technological platform using both Q-View<sup>™</sup>  
240 and Quansys Software. Sensitivity ranges between 1 pg/mL and 30 pg/mL depending  
241 on the considered analyte.

### 242 **2.9. Specific cytokine/chemokine production: ELISA analysis**

243 Two cytokines and one chemokine were assessed using Human DuoSet ELISA (R&D  
244 Systems, Minneapolis, MN, USA) interleukin 1 $\alpha$  (IL-1 $\alpha$ /IL-1F1, #DY200), interleukin  
245 8 (IL-8/CxCL8, #DY208) and RANTES (CCL5/RANTES, #DY278). Absorbance was  
246 determined using an ELISA-reader (Multiskan<sup>®</sup> EX, Thermo Scientific, Waltham, MA,  
247 USA) at 450 nm and 540 nm to correct the optical imperfections in the plate.  
248 Calibration curves were calculated using Ascent Software<sup>®</sup> (Thermo Fisher Scientific,  
249 Waltham, MA, USA). Concentrations are expressed in pg/mL and the lower limits of  
250 quantification are 31.26, 7.81, 156 pg/mL for IL-8, IL-1 $\alpha$ , and RANTES, respectively.

### 251 **2.10. Statistical analysis**

252 All results are reported as mean  $\pm$  standard deviation. Except for Q-Plex<sup>™</sup> analysis that  
253 was performed only once with duplicated quantification, all other experiments were  
254 performed at least in two independent experiments, each with duplicated quantification.  
255 The exact number of independent experiments (n) is indicated in the legend of the  
256 figures. After verifying the Normal distribution of results using the Shapiro-Wilk test  
257 ( $p < 0.05$ ), statistical differences were analyzed using one-way ANOVA followed by  
258 Tukey HSD (Honestly Significant Difference) test.  $p < 0.05$  was considered significant.

## 259 **3. Results**

### 260 **3.1. RHE functionality upon exposure to pollutants**

261 RHEs were exposed to various environmental pollutants: two PM<sub>0.3-2.5</sub> samples – PMm,  
262 rich in metals and inorganic elements, and PMo, rich in organic compounds – two VOC  
263 mixtures – VOCwb, emanating from a water-based paint, and VOCsb, from a solvent-  
264 based paint – and TS.

265 Results of the MTT assay (Fig. 2) reveals that the pollutant which most affects RHE is  
266 TS, inducing a significant -43.9% (p<0.0001) decrease in cell functionality compared to  
267 the negative control. Moreover, both PM were found to alter the functionality of RHEs.  
268 The effect is dose-dependent and statistically significant from the lowest exposure doses  
269 to 3 µg/cm<sup>2</sup> of PMm (-10.5%, p=0.0155) or 15 µg/cm<sup>2</sup> of PMo (-15.4%, p<0.0001). The  
270 negative effect is higher when RHEs are exposed to PMm than to PMo,  
271 reaching -39.4% (p<0.0001) for exposure to 30 µg/cm<sup>2</sup> of PMm, while the decrease  
272 induced by PMo is of -26.7% (p<0.0001). Among the two VOCs tested, only VOCsb  
273 affects RHEs, leading to -8.7% (p=0.0213) in cell functionality, the -4.4% decrease  
274 induced by VOCwb being not significant (p=0.4543).

### 275 **3.2. RHE functionality upon preconditioning in a semi-dry or humid airflow** 276 ***followed by exposure to pollutants***

277 To evaluate the impact of airflow with different relative humidity on the effect of  
278 pollutants, we preconditioned RHEs by submitting them to a semi-dry (45% relative  
279 humidity – RH) or a humid (90% RH) airflow for 2 hours prior exposure to pollutants.  
280 Controls included negative controls, preconditioned by the semi-dry or humid airflow  
281 but not subjected to pollutants, and RH controls, incubated with pollutants but not to

282 preconditioning by the humid/semi-dry airflow (kept in the incubator at 37°C with 90%  
283 RH).

284 Results (Fig. 3) showed that, for the negative control, preconditioning by the humid  
285 airflow does not affect RHE compared to the RH control. This lack of effect of  
286 preconditioning by the humid airflow is also observed when comparing RHE incubated  
287 with pollutants with their respective RH controls. Only preconditioning by the semi-dry  
288 airflow affects the results of the MTT test for both, the negative control and the RHE  
289 treated with the various pollutants. The decrease is always significant when results are  
290 compared to that of RHE preconditioned by the humid airflow and almost always when  
291 compared to the respective RH controls (the exception being PM<sub>m</sub>). Still, within series,  
292 the decrease in cellular functionality induced by the semi-dry preconditioning compared  
293 to preconditioning by the humid airflow remains generally mild (negative control: -  
294 12.9%, p=0.0443; PM<sub>m</sub>: -16.7%, p=0.0242; PM<sub>o</sub>: -19.8%, p=0.0014; VOC<sub>wb</sub>: -23.9%,  
295 p<0.0001; VOC<sub>sb</sub>: -26.6%, p<0.0001), except for TS for which it reaches -34.1%  
296 (p=0.0007).

### 297 **3.3. Inflammatory response upon exposure to pollutants**

298 We have then investigated the inflammatory response induced by pollutants by  
299 monitoring the production of nine cytokines (IL-1 $\alpha$ , IL-1 $\beta$ , IL-2, IL-4, IL-6, IL-8,  
300 IL-10, IFN $\alpha$ , TNF $\alpha$ ) and eight chemokines (Eotaxin, GRO $\alpha$ , I-309, IP-10, MCP-1,  
301 MCP-2, RANTES, TARC). The results are presented in Fig. 4.

302 IL-1 $\alpha$ , IL-6, IL-8, and RANTES are the only cytokines/chemokines almost  
303 systematically and significantly induced by a factor of 1.3 to 2.7 by pollutants: PM at  
304 15  $\mu\text{g}/\text{cm}^2$  and over, VOCs and TS. Even if VOC<sub>wb</sub> does not significantly induce  
305 IL-1 $\alpha$ /IL-6 and TS does not significantly induce IL-8, the probabilities are at the limit of



306 significance for IL-1 $\alpha$  and VOCwb (p=0.0535), as well as for IL-8 and TS (p=0.0903).  
307 For both PM a dose-dependent effect is clearly observed for IL-1 $\alpha$ , IL-6, IL-8, and  
308 RANTES. Besides, the induction of the three cytokines/chemokines seems to be higher  
309 for PMm (x2.2 folds for IL-1 $\alpha$ , x2.7 folds for IL-6, x2.7 folds for IL-8 and 2.1 folds for  
310 RANTES with 30  $\mu\text{g}/\text{cm}^2$ ) than for PMo (x2.1 folds for IL-1 $\alpha$ , x1.9 folds for IL-6, x2.1  
311 folds for IL-8 and 1.8 folds for RANTES with 30  $\mu\text{g}/\text{cm}^2$ ).  
312 In these experimental series, none of the pollutants induced IL-1 $\beta$ , IL-4, Eotaxin, I-309,  
313 MCP-2 or TARC, and the induction of IL-2, IL-10, IFN $\alpha$ , TNF $\alpha$ , GRO $\alpha$ , IP-10, MCP-1  
314 depends on the pollutant. Still, overall PMm is the pollutant inducing the most  
315 cytokines and chemokines (10 among the 17 tested) while VOCwb is the one inducing  
316 the least (5), VOCsb, and TS being intermediate.

317 ***3.4. Inflammatory response upon preconditioning in a semi-dry or humid airflow***  
318 ***followed by exposure to pollutants***

319 To analyze the effect of airflows with different relative humidity on the inflammatory  
320 response induced by pollutants, we preconditioned RHEs for two hours using a semi-  
321 dry or humid airflow before subjecting them to pollutants. For this analysis, we focused  
322 on IL-1 $\alpha$ , IL-8, and RANTES that were induced by most pollutants tested. Similarly to  
323 the study of the cellular functionality of both, semi-dry/humid airflow and pollutants,  
324 the controls encompassed negative controls, subjected to preconditioning by the  
325 different airflows but not to pollutants, and RH controls, subjected to pollutants but not  
326 to preconditioning by the airflows. The results are presented in Fig. 5.

327 In the negative controls, comparison of the amount of cytokines/chemokine released by  
328 the RH controls and by RHEs preconditioned by the 90% RH airflow shows that  
329 preconditioning by the humid airflow significantly increases the release of IL-1 $\alpha$  and

330 IL-8 by a factor of 1.9, while, for RANTES, the increase is not significant. The increase  
331 in IL-1 $\alpha$  and IL-8 is also observed when comparing RH controls treated with pollutants  
332 and RHEs which underwent both, preconditioning by the humid airflow and incubation  
333 with pollutants, but, in that case, the increase is also significant for RANTES. In  
334 addition, the fold change compared to RHE treated with pollutants but not  
335 preconditioned by the humid airflow is much higher, reaching over 10 folds for IL-8  
336 induction by any of the PM and 3 to 5 folds for RANTES inductions by whatever  
337 VOCs.

338 For all negative controls, preconditioning in the semi-dry airflow significantly increases  
339 the release of IL-1 $\alpha$ , IL-8 and RANTES compared to the RH controls. Except for IL-1 $\alpha$ ,  
340 this increase is significantly higher than that obtained upon preconditioning by the  
341 humid airflow. When RHEs are treated with both, preconditioning by the semi-dry  
342 airflow and either PM, the release of IL-1 $\alpha$ , IL-8 and RANTES is higher than in the RH  
343 controls, but overall significantly lower than when RHEs are preconditioned by the  
344 humid airflow. For TS, combination with preconditioning by the semi-dry airflow acts  
345 similarly to PM on IL-1 $\alpha$ , IL-8, and RANTES. Contrary to PM and TS, preconditioning  
346 by the semi-dry airflow and either VOC, VOC<sub>wb</sub>, or VOC<sub>sb</sub>, leads to an increase in  
347 IL-1 $\alpha$ , IL-8, and RANTES compared to preconditioning by the humid airflow.

#### 348 **4. Discussion**

349 In recent years, several studies were devoted to the biological effect of air pollutants.  
350 Many focused on small particulate matters ( $PM_{<2.5}$ ) due to their role in pulmonary  
351 morbidity and mortality. But PM are not the only source of air pollution and, with the  
352 increasing time spent inside, VOCs are also important to consider. Besides, the majority  
353 of the studies focuses on the pulmonary epithelium. Little is known about the fate of the  
354 skin despite the fact it is the largest human organ and it is also constantly exposed to the  
355 environment. Therefore, we wanted to better understand the impact of air pollutants on  
356 the skin and, especially, to investigate how an environmental factor such as humidity  
357 affects the response to pollutants knowing that changes in relative humidity are  
358 sufficient to impact the skin (Singh and Maibach, 2013; Cau et al., 2017).

359 Among the pollutants we tested, TS was primarily used as a positive control. This  
360 pollutant is a complex mixture containing over 4,000 gaseous and particulate  
361 compounds, including VOCs and PM. Its effect on premature skin aging is already well  
362 documented and we previously showed, using the very same RHE system, that it  
363 induces morphological alterations, oxidative stress, leading to the production of  
364 inflammatory cytokines (Lecas et al., 2016). Therefore, our primary interest was the  
365 response induced by two types of pollutants, fine particles ( $PM_{0.3-2.5}$ ) and VOCs, with  
366 two different samples for each. Both PM samples present similar granulometric profiles,  
367 but show very different chemical compositions, therefore enabling us to evaluate the  
368 impact of chemicals adsorbed to the particles. PMm are originating from a highly  
369 polluted urban region of Sub-Saharan Africa (Cotonou, Benin). They are characterized  
370 by their extreme richness in metallic elements as the region where they were collected is  
371 surrounded by soils with high concentrations of iron oxide, aluminum oxide, and heavy

372 metals (Cachon et al., 2014). On the contrary, PM<sub>10</sub> are from a region of France  
373 (Dunkerque) with intense industrial activities and heavy vehicle traffic, which their  
374 richness in organic compounds reflects (Dergham et al., 2015). The last two pollutants  
375 we tested are VOCs. Much less studied, we focused on VOCs from a solvent-based  
376 paint that was manufactured before the French regulation limiting VOCs in construction  
377 and decoration products and that liberates large amounts of various VOCs. The second  
378 source of VOCs is a recent water-based paint manufactured after the French regulation  
379 and showing reduced VOCs emissions.

380 All these pollutants are real environmental pollutants. In addition, the exposure system  
381 we set up is realistic in the sense that the pollutants are delivered to the apical side of  
382 RHEs, therefore mimicking a real-life situation. Still, it is inhomogeneous in its  
383 exposition due to the physical nature of the different pollutants tested. As a matter of  
384 fact, PM are applied topically and remain on RHE for 24 hours before analysis, making  
385 it a static system. On the other hand, VOCs are delivered dynamically, via a one-hour  
386 airflow followed by a 24-hours incubation before analysis. The system we used for TS  
387 is intermediate. Fresh TS is generated in a chamber where its compounds are allowed to  
388 interact with, and sediment onto RHEs. Therefore, it is more of a static system that  
389 favors the action of the PM constituents that will stay on RHEs, rather than that of its  
390 gaseous phase for which the contact is time-limited. Another source of inhomogeneity is  
391 the dose of pollutants tested. If the doses of PM and TS we tested are much higher than  
392 normal exposures, as frequently in *in vitro* studies, those of VOCs are, on the contrary,  
393 very low: 6.1 µg/liter for VOC<sub>wb</sub> and 183.5 µg/liter for VOC<sub>sb</sub>, therefore 0.73 µg and  
394 22.0 µg respectively during the one-hour exposure. These low doses are due to the fact  
395 that we followed the ISO standards to generate the VOCs samples.

396 Not only does our experimental setup show heterogeneity in the testing of pollutants,  
397 but the pollutants we tested are very different and interact differently with the skin. PM  
398 are a complex mixture of insoluble particles – the physical part – and soluble  
399 components absorbed to their surface – the chemical part. If PM can induce their effects  
400 through the release of soluble components that can enter the stratum corneum, the  
401 tiniest PM can enter the skin. Indeed, Jin et al. (2018) showed that PM can enter the  
402 skin by accumulating in hair follicles and sweat glands. In RHE, they were found to  
403 enter the upper layers in less than 24 hours (Magnani et al., 2015), which is not  
404 surprising regarding the fact that PM break the skin barrier by down-regulating  
405 filaggrin, thereby disrupting the tight skin junctions (Pan et al., 2015; Lee et al., 2016).  
406 RHEs are deprived of hair follicles and sweat glands, but we incubated them with PM  
407 for 24 hours. Therefore, it seems likely that the toxicological endpoint we observe is  
408 due to both, the prolonged contact and/or diffusion of soluble components through the  
409 surface of the stratum corneum, as well as to the direct release of compounds absorbed  
410 to their surface within the upper layers of RHE. On their side, VOCs must have directly  
411 diffused into the upper layers of RHE. Indeed, the toxicity of hexane and toluene, two  
412 VOCs, relates to their lipophilicity and their accumulation in the lipid bilayer of cellular  
413 membranes (Dreiem et al., 2003; Pariselli et al., 2009). Besides, VOCs are also known  
414 to affect the skin due to the ability of UV and NO<sub>x</sub> to transform them into  
415 photochemical oxidants, which seems unlikely to have played a major role considering  
416 our experimental setup.

417 Whatever the entry route of the pollutants, inhibition of the succinate dehydrogenase  
418 revealed by the MTT assay shows that PM, TS, and VOCsb affect RHEs. For the two  
419 PM, the alteration is dose-dependent, and the effect is stronger when RHE are treated

420 with PMm than with PMo. This may result from the high level of transition metals and  
421 other metals adsorbed on PMm (*e.g.* Al, Cu, Fe, Mn, Zn, Pb, *etc.*) that are powerful  
422 ROS inducers. Using the same exposure system, we previously showed that PMm are  
423 powerful inducers of oxidative stress (Verdin et al., 2019). The fact that polycyclic  
424 aromatic hydrocarbons adsorbed to PM bind the aryl hydrocarbon receptor (AhR) to  
425 induce a signaling pathway leading to ROS formation and proinflammatory gene  
426 expression is now well established (Esser et al., 2018; Parrado et al., 2019). Oxidative  
427 stress was also demonstrated for PMo using BEAS-2B bronchial epithelial cells  
428 (Dergham et al., 2015). Evidence of oxidative stress was also found for keratinocytes  
429 exposed to different VOCs (Dezest et al., 2017). Oxidative stress and inflammation are  
430 tightly linked and, if ROS are not controlled, they lead to inflammatory cell and/or  
431 tissue injury (Lonkar and Dedon, 2010). In our case, all pollutants tested induce  
432 RANTES and almost all of them IL-1 $\alpha$  as well as IL-8. Similarly to the cellular  
433 functionality, the effect is more pronounced for PMm, which also induces more  
434 cytokines and chemokines, than PMo. The induction of cytokines and chemokines  
435 production is also observed with the two VOCs and TS even if the range of cytokines  
436 and chemokines induced is more limited, especially for VOCwb.

437 When testing the influence of preconditioning by a humid *versus* a semi-dry airflow,  
438 results show that the semi-dry airflow impacts cellular functionality, whatever pollutant  
439 tested. Negative controls also revealed increased levels of IL-8 and RANTES upon  
440 preconditioning by the semi-dry airflow. If airflows differ between them by their  
441 relative humidity, they also differ from the negative control by the temperature (24°C).  
442 Still, RHEs are maintained at 37°C and it is only their apical side that is subjected to  
443 this lower temperature. Hence, it sounds reasonable to assume that most of the effect we

444 observed is due to the differences in relative humidity, and that the increased levels of  
445 IL-8 and RANTES could be the first consequence of the initial increase in  
446 Transepidermal Water Loss (TEWL) followed by inflammatory cytokine stimulation as  
447 described in studies performed in dry conditions (Singh and Maibach, 2013). Still,  
448 results show that the short preconditioning period in semi-dry or humid air is sufficient  
449 to affect the reaction of RHE towards pollutants. Contrary to cellular functionality, the  
450 different preconditioning is also sufficient to reveal different effects depending on the  
451 type of pollutants. For both PM and TS, preconditioning by the semi-dry airflow tends  
452 to decrease the levels of IL-1 $\alpha$ , IL-8, and RANTES compared to preconditioning by the  
453 humid airflow. The situation is just the opposite for the induction of IL-1 $\alpha$ , IL-8, and  
454 RANTES by the two VOCs. Strikingly, both VOCs induce an almost identical response  
455 despite their very different qualitative and quantitative compositions. This response is  
456 similar to that of the negative control and suggests that, under the conditions used (low  
457 doses and short exposure), the effect of preconditioning by the semi-dry airflow primes  
458 over the response to VOCs. Taken together, these results suggest that the response of  
459 the skin to RH is the main driver of the toxicological endpoint and that its outcome  
460 depends mainly on the physical nature of the pollutant.

461 Several works studied the effect of dry conditions on the skin (reviewed in Engebretsen  
462 et al., 2016; Goad and Gawkrödger, 2016). They show that human skin placed in dry  
463 conditions presents an increased stratum corneum thickness, an increased TEWL, a  
464 reduced elasticity, and an increased susceptibility to mechanical stress. In hairless mice,  
465 dry condition (3 days at 10% RH) induces reduced desmosomal degradation that was  
466 attributed to the reduced water content of the stratum corneum, leading to impaired  
467 desquamation and a scaly surface (Sato et al., 1998). Furthermore, the amount of IL-1 $\alpha$

468 was found higher in mice kept under dry conditions (Ashida et al., 2001). RHE  
469 produced in semi-dry conditions (30-50% RH) also show increased TEWL, a thicker  
470 stratum corneum, and an increased level of epidermal protein deimination. These  
471 alterations lead to the breakdown of filaggrin, a filament-associated protein that binds to  
472 keratin fibers in epithelial cells (Cau et al., 2017). If all these works pinpoint at a barrier  
473 deficit when the skin is subjected to dry conditions, one should be cautious in  
474 extrapolating them to our study. Most of the works mentioned above were performed  
475 comparing much longer incubation times in different RH conditions than the two hours  
476 preconditioning time we used. In our case, preconditioning by the semi-dry airflow  
477 might have only led to the very first step of the above-mentioned changes: the increased  
478 water loss, the beginning of the dehydration of the upper layers of the stratum corneum  
479 and, as we show it, the release of cytokines/chemokines. Therefore, for VOCs the effect  
480 we observe would be driven by our dynamic experimental setup and would only reflect  
481 the effect of the two hours preconditioning in semi-dry conditions.

482 The fate of PM would be different but can also be explained by the mechanical  
483 characteristics of the skin under the different RH conditions. In that respect, the static  
484 experimental design we used for TS reflects the particulate nature of TS rather than that  
485 of its gaseous part since it induces a similar response than PM. Two mutually none  
486 exclusive aspects could explain the lower cytokine/chemokine induction observed upon  
487 preconditioning by the semi-dry airflow compared to the humid airflow. The first one is  
488 that, as mentioned above, the semi-dry airflow rapidly lead to dehydration of the upper  
489 layer of the stratum corneum and a scaly surface. These could have limited the contacts  
490 between PM and RHE and/or limited the diffusion of the chemical components  
491 absorbed to the surface of PM. On the other hand, preconditioning under humid



492 conditions might have favored these contacts. Using transmission and cryo-scanning  
493 electron microscopy, Warner et al. (2013) show that a four-hours treatment in an  
494 atmosphere saturated with water leads to a three-fold increase in the thickness of the  
495 stratum corneum with large pools of water accumulating in intercellular spaces where  
496 the lipid structures are disrupted. This study was performed *in vivo*, on the volar  
497 forearm of volunteers. With the weaker stratum corneum of RHE, we can assume that  
498 such an effect can occur when they are maintained under 90% RH. Not only would it  
499 explain better contact between PM and the upper cell layers, but the rupture of the  
500 stratum corneum barrier and the large pool of water might lead to an increased entry of  
501 PM. It would also explain a better diffusion of the metallic elements absorbed to the  
502 surface of PMm and, therefore, the stronger release of IL-1 $\alpha$ , IL-8, and RANTES.

503 It is important to note that our conclusions are quite limited by the fact that the  
504 experiments were performed on a single batch of RHE which are known to show some  
505 inter-batch variability. A last limitation is due to the short period during which RHE can  
506 be used. This restricts the use of our system to the test of short exposure periods and  
507 precludes us from testing chronic like exposure. Still, the use of a 3D-skin model – a  
508 reconstructed human epidermis – enabled us to mimic the effects of close contact  
509 between pollutants and the skin. The experimental system we set up also allowed us to  
510 test realistic environmental pollutants. Not only are they realistic in their generation  
511 and, by extension, in their physicochemical composition but, also, in the way we  
512 delivered them to RHE, which reflects the real human dermal exposure route: an air-  
513 liquid exposure resulting in the topical application of pollutants. Finally, the use of the  
514 innovative humidification station has proven to be suitable, and the conditions we tested

515 are representative of real environmental conditions, since the 2 hours preconditioning is  
516 sufficient to induce different reactions towards various environmental pollutants.

## 517 **Conclusion**

518 In the course of this study, we tested various pollutants with different chemical  
519 compositions, applying them to the apical side of RHE and being particularly interested  
520 in the effect relative humidity has on the reaction to pollutants. The negative effect of  
521 pollutants on the cellular functionality is aggravated when RHE are preconditioned for  
522 two hours by a semi-dry airflow. Investigating several cytokines and chemokines, we  
523 showed that IL-1 $\alpha$ , IL-6, IL-8, and RANTES are the cytokines/chemokines almost  
524 systematically induced by most pollutants. When RHE are preconditioned by a semi-  
525 dry/humid airflow before being subjected to pollutants, the release of IL-1 $\alpha$ , IL-8, and  
526 RANTES falls into two groups. For VOCs, preconditioning by a semi-dry airflow  
527 exacerbates IL-1 $\alpha$ , IL-8, and RANTES release, similar to what happens in the absence  
528 of pollutants, indicating a response driven by RH rather than by VOCs. On the other  
529 hand, for PM and TS, preconditioning by a semi-dry airflow leads to a decrease in the  
530 release of IL-1 $\alpha$ , IL-8, and RANTES. Our interpretation is that the effect of RH on the  
531 skin structure primes over the chemical composition of the pollutants. It is the changes  
532 induced by the different humidity conditions – and our experimental design – that  
533 determine the outcome of the toxicological endpoint of a pollutant depending on its  
534 physical nature.

535 **Declaration of interest**

536 The authors declare no conflict of interest.

537

538 **CRedit authorship contribution statement**

539 **Emeline Seurat:** Conceptualization, Methodology, Formal analysis, Writing-original  
540 draft. **Anthony Verdin:** Conceptualization, Methodology, Formal analysis,  
541 Investigation, Proof-reading. **Fabrice Cazier:** Conceptualization, Methodology, Formal  
542 analysis, Investigation, Proof-reading. **Dominique Courcot:** Supervision, Proof-  
543 reading. **Richard Fitoussi:** Funding acquisition, Supervision, Proof-reading. **Katell**  
544 **Vié:** Funding acquisition, Proof-reading. **Valérie Desauziers:** Methodology, Formal  
545 analysis, Supervision, Proof-reading. **Isabelle Momas:** Supervision, Proof-reading.  
546 **Nathalie Seta:** Supervision, Proof-reading. **Sophie Achard:** Conceptualization,  
547 Methodology, Formal analysis, Investigation, Writing-original draft, Visualization,  
548 Ressources, Data curation, Funding Acquisition, Supervision.

549

550 **Acknowledgments**

551 The authors thank Dr. Gallic Beauchef for helpful discussions and comments. They also  
552 wish to thank Dr. Philippe Crouzet, Estium-Concept, for scientific writing services.

553 **References**

- 554 Ashida, Y., Ogo, M., Denda, M., 2001. Epidermal Interleukin-1 $\alpha$  Generation Is  
555 Amplified at Low Humidity: Implications for the Pathogenesis of Inflammatory  
556 Dermatoses. *Br J Dermatol.* 144, 238-243. [https://doi.org/10.1046/j.1365-](https://doi.org/10.1046/j.1365-2133.2001.04007.x)  
557 [2133.2001.04007.x](https://doi.org/10.1046/j.1365-2133.2001.04007.x)
- 558 Auer, R., Concha-Lozano, N., Jacot-Sadowski, I., Cornuz, J., Berthet, A., 2017. Heat-  
559 Not-Burn Tobacco Cigarettes: Smoke by Any Other Name. *JAMA Intern Med.* 177,  
560 1050-1052. <https://doi.org/10.1001/jamainternmed.2017.1419>
- 561 Badji, C., Beigbeder, J., Garay, H., Bergeret, A., Bénézet, J.C., Desauziers, V., 2018.  
562 Under glass weathering of hemp fibers reinforced polypropylene biocomposites: Impact  
563 of Volatile Organic Compounds emissions on indoor air quality. *Polym Degrad Stabil.*  
564 149, 85-95. <https://doi.org/10.1016/j.polymdegradstab.2018.01.020>
- 565 Bardet, G., Mignon, V., Momas, I., Achard, S., Seta, N., 2016. Human Reconstituted  
566 Nasal Epithelium, a promising *in vitro* model to assess impacts of environmental  
567 complex mixtures. *Toxicol In Vitro.* 32, 55-62. <http://doi.org/10.1016/j.tiv.2015.11.019>
- 568 Beelen, R., Raaschou-Nielsen, O., Stafoggia, M., Andersen, Z.J., Weinmayr, G.,  
569 Hoffmann, B., Wolf, K., Samoli, E., Fischer, P., Nieuwenhuijsen, M., Vineis, P., Xun,  
570 W.W., Katsouyanni, K., Dimakopoulou, K., Oudin, A., Forsberg, B., Modig, L.,  
571 Havulinna, A.S., Lanki, T., Turunen, A., Oftedal, B., Nystad, W., Nafstad, P., De Faire,  
572 U., Pedersen, N.L., Ostenson, C.G., Fratiglioni, L., Penell, J., Korek, M., Pershagen, G.,  
573 Eriksen, K.T., Overvad, K., Ellermann, T., Eeftens, M., Peeters, P.H., Meliefste, K.,  
574 Wang, M., Bueno-de-Mesquita, B., Sugiri, D., Kramer, U., Heinrich, J., de Hoogh, K.,  
575 Key, T., Peters, A., Hampel, R., Concini, H., Nagel, G., Ineichen, A., Schaffner, E.,  
576 Probst-Hensch, N., Kunzli, N., Schindler, C., Schikowski, T., Adam, M., Phuleria, H.,

577 Vilier, A., Clavel-Chapelon, F., Declercq, C., Grioni, S., Krogh, V., Tsai, M.Y., Ricceri,  
578 F., Sacerdote, C., Galassi, C., Migliore, E., Ranzi, A., Cesaroni, G., Badaloni, C.,  
579 Forastiere, F., Tamayo, I., Amiano, P., Dorronsoro, M., Katsoulis, M., Trichopoulou,  
580 A., Brunekreef, B., Hoek, G., 2014. Effects of long-term exposure to air pollution on  
581 natural-cause mortality: an analysis of 22 European cohorts within the multicentre  
582 ESCAPE project. *Lancet*. 383, 785-795. [https://doi.org/10.1016/S0140-6736\(13\)62158-](https://doi.org/10.1016/S0140-6736(13)62158-3)  
583 [3](https://doi.org/10.1016/S0140-6736(13)62158-3)  
584 Cachon, B.F., S. Firmin, S., Verdin, A., Ayi-Fanou, L., Billet, S., Cazier, F., Martin,  
585 P.J., Aissi, F., Courcot, D., Sanni, A., Shirali, P., 2014 Proinflammatory effects and  
586 oxidative stress within human bronchial epithelial cells exposed to atmospheric  
587 particulate matter (PM<sub>2.5</sub> and PM<sub>>2.5</sub>) collected from Cotonou, Benin. *Environ Pollut.*  
588 185, 340-351. <https://doi.org/10.1016/j.envpol.2013.10.026>  
589 Cau, L., Pendaries, V., Lhuillier, E., Thompson, P.R., Serre, G., Takahara, H., Mechin,  
590 M.C., Simon, M., 2017. Lowering relative humidity level increases epidermal protein  
591 deimination and drives human filaggrin breakdown. *J Dermatol Sci*. 86, 106-113.  
592 <https://doi.org/10.1016/j.jdermsci.2017.02.280>  
593 Dergham, M., Lepers, C., Verdin, A., Cazier, F., Billet, S., Courcot, D., Shirali, P.,  
594 Garçon, G., 2015. Temporal-spatial variations of the physicochemical characteristics of  
595 air pollution Particulate Matter (PM<sub>2.5-0.3</sub>) and toxicological effects in human  
596 bronchial epithelial cells (BEAS-2B). *Environ Res*. 137, 256-267.  
597 <https://doi.org/10.1016/j.envres.2014.12.015>  
598 Desauziers, V., Auguin, B., 2012. SPME-adaptor: a rapid sampling for the analysis of  
599 VOCs traces in air. *Techniques de l'ingénieur Innovations en analyses et mesures*,  
600 in149.

601 Dezeit, M., Le Behec, M., Chavatte, L., Desauziers, V., Chaput, B., Grolleau, J.L.,  
602 Descargues, P., Nizard, C., Schnebert, S., Lacombe, S., Bulteau, A.L., 2017. Oxidative  
603 damage and impairment of protein quality control systems in keratinocytes exposed to a  
604 volatile organic compounds cocktail. *Sci Rep.* 7, 10707. [https://doi.org/10.1038/s41598-](https://doi.org/10.1038/s41598-017-11088-1)  
605 [017-11088-1](https://doi.org/10.1038/s41598-017-11088-1)

606 Dreiem, A., Myhre, O., Fonnum, F., 2003. Involvement of the extracellular signal  
607 regulated kinase pathway in hydrocarbon-induced reactive oxygen species formation in  
608 human neutrophil granulocytes. *Toxicol Appl Pharmacol* 190, 102-110.  
609 [https://doi.org/10.1016/S0041-008X\(03\)00158-3](https://doi.org/10.1016/S0041-008X(03)00158-3)

610 Engebretsen, K.A., Johansen, J.D., Kezic, S., Linneberg, A., Thyssen, J.P., 2016. The  
611 Effect of Environmental Humidity and Temperature on Skin Barrier Function and  
612 Dermatitis. *J Eur Acad Dermatol Venereol.* 30, 223-249.  
613 <https://doi.org/10.1111/jdv.13301>

614 Esser, C. , Lawrence, B.P., Sherr, D.H., Perdew, G.H., Puga, A. , Barouki, R., Coumoul,  
615 X., 2018. Old Receptor, New Tricks - The Ever-Expanding Universe of Aryl  
616 Hydrocarbon Receptor Functions. Report From the 4th AHR Meeting, 29-31 August  
617 2018 in Paris, France. *Int J Mol Sci.* 19, 3603. <https://doi.org/10.3390/ijms19113603>

618 European Union, 2010. Directive 2010/75/EC of the European Parliament and of the  
619 Council of 24 November 2010 on industrial emissions (integrated pollution prevention  
620 and control). *Off J Eur Union.* 334, 17-119.

621 Flament, F., Bazin, R., Laquieze, S., Rubert, V., Simonpietri, E., Piot, B., 2013. Effect  
622 of the sun on visible clinical signs of aging in Caucasian skin. *Clin Cosmet Investig*  
623 *Dermatol.* 6, 221-232. <https://doi.org/10.2147/CCID.S44686>

624 Goad, N., Gawkrödger, D.J., 2016. Ambient Humidity and the Skin: The Impact of Air  
625 Humidity in Healthy and Diseased States. *J Eur Acad Dermatol Venereol.* 30, 1285-  
626 1294. <https://doi.org/10.1111/jdv.13707>

627 Haydont, V., Bernard, B.A., Fortunel, N.O., 2019. Age-related evolutions of the dermis:  
628 Clinical signs, fibroblast and extracellular matrix dynamics. *Mech Ageing Dev.* 177,  
629 150-156. <https://doi.org/10.1016/j.mad.2018.03.006>

630 Hoek, G., Krishnan, R.M., Beelen, R., Peters, A., Ostro, B., Brunekreef, B., Kaufman,  
631 J.D., 2013. Long-term air pollution exposure and cardio-respiratory mortality: a review.  
632 *Environ Health.* 12, 43. <https://doi.org/10.1186/1476-069X-12-43>

633 Hoffmann, D., Djordjevic, M.V., Hoffmann, I., 1997. The Changing Cigarette. 26, 427-  
634 434. <https://doi.org/10.1006/pmed.1997.0183>

635 International Organization for Standardization (ISO), 2006a. ISO 16000-9:2006 -  
636 Indoor air – Part 9: Determination of the emission of volatile organic compounds from  
637 building products and furnishing - Emission test chamber method. Accessed 20 July  
638 2020. <https://www.iso.org/standard/38203.html>

639 International Organization for Standardization (ISO), 2006b. ISO 16000-11:2006 -  
640 Indoor air – Part 11: Determination of the emission of volatile organic compounds from  
641 building products and furnishing - Sampling, storage of samples and preparation of test  
642 specimens. Accessed 20 July 2020. <https://www.iso.org/standard/38205.html>

643 Jackson, R., 2001. Elderly and sun-affected skin. Distinguishing between changes  
644 caused by aging and changes caused by habitual exposure to sun. *Can Fam Physician.*  
645 47, 1236-1243.

646 Jin, S.P., Li, Z., Choi, E.K., Lee, S., Kim, Y.K., Seo, E.Y., Chung, J.H., Cho, S., 2018.  
647 Urban particulate matter in air pollution penetrates into the barrier-disrupted skin and



648 produces ROS-dependent cutaneous inflammatory response *in vivo*. J Dermatol Sci. 91,  
649 175-183. <https://doi.org/10.1016/j.jdermsci.2018.04.015>

650 Kostianen, R., 1995. Volatile organic compounds in the indoor air of normal and sick  
651 houses. Atmos Environ. 29, 693-702. [https://doi.org/10.1016/1352-2310\(94\)00309-9](https://doi.org/10.1016/1352-2310(94)00309-9)

652 Krutmann, J., Liu, W., Li, L., Pan, X., Crawford, M., Sore, G., Seite, S., 2014. Pollution  
653 and skin: from epidemiological and mechanistic studies to clinical implications. J  
654 Dermatol Sci. 76, 163-168. <https://doi.org/10.1016/j.jdermsci.2014.08.008>

655 Lecas, S., Boursier, E., Fitoussi, R., Vie, K., Momas, I., Seta, N., Achard, S., 2016. *In*  
656 *vitro* model adapted to the study of skin ageing induced by air pollution. Toxicol Lett.  
657 259, 60-68. <https://doi.org/10.1016/j.toxlet.2016.07.026>

658 Lee, C.W., Lin, Z.C., Hu, S.C., Chiang, Y.C., Hsu, L.F., Lin, Y.C., Lee, I.T., Tsai,  
659 M.H., Fang, J.Y., 2016. Urban particulate matter down-regulates filaggrin via COX2  
660 expression/ PGE2 production leading to skin barrier dysfunction. Sci Rep. 6, 27995.  
661 <https://doi.org/10.1038/srep27995>

662 Löfrth, G., 1989. Environmental Tobacco Smoke: Overview of Chemical Composition  
663 and Genotoxic Components. Mutat Res. 222, 73-80. [https://doi.org/10.1016/0165-](https://doi.org/10.1016/0165-1218(89)90021-9)  
664 [1218\(89\)90021-9](https://doi.org/10.1016/0165-1218(89)90021-9)

665 Lonkar, P., Dedon, P.C., 2011. Reactive Species and DNA Damage in Chronic  
666 Inflammation: Reconciling Chemical Mechanisms and Biological Fates. Int J Cancer.  
667 128, 1999-2009. <https://doi.org/10.1002/ijc.25815>

668 Loomis, D., Huang, W., Chen, G., 2014. The International Agency for Research on  
669 Cancer (IARC) evaluation of the carcinogenicity of outdoor air pollution: focus on  
670 China. Chin J Cancer. 33, 189-196. <https://doi.org/10.5732/cjc.014.10028>

671 Magnani, N.D., Muresan, X.M., Belmonte, G., Cervellati, F., Sticozzi, C., Pecorelli, A.,  
672 Miracco, C., Marchini, T., Evelson, P., Valacchi, G., 2016. Skin damage mechanisms  
673 related to airborne particulate matter exposure. *Toxicol Sci.* 149, 227-236.  
674 <https://doi.org/10.1093/toxsci/kfv230>

675 Makrantonaki, E., Vogel, M., Scharffetter-Kochanek, K., Zouboulis, C.C., 2015. [Skin  
676 aging: Molecular understanding of extrinsic and intrinsic processes]. *Hautarzt.* 66, 730-  
677 737. <https://doi.org/10.1007/s00105-015-3692-z>

678 Morita, A., 2007. Tobacco smoke causes premature skin aging. *J Dermatol Sci.* 48, 169-  
679 175. <https://doi.org/10.1016/j.jdermsci.2007.06.015>

680 Ortiz, A., Grando, S.A., 2012. Smoking and the skin. *Int J Dermatol.* 51, 250-262.  
681 <https://doi.org/10.1111/j.1365-4632.2011.05205.x>

682 Pan, T.L., Wang, P.W., Aljuffali, I.A., Huang, C.T., Lee, C.W., Fang, J.Y., 2015. The  
683 impact of urban particulate pollution on skin barrier function and the subsequent drug  
684 absorption. *J Dermatol Sci.* 78, 51–60. <https://doi.org/10.1016/j.jdermsci.2015.01.011>

685 Pariselli, F., Sacco, M. G., Ponti, J., Rembges, D., 2009. Effects of toluene and benzene  
686 air mixtures on human lung cells (A549). *Exp Toxicol Pathol* 61, 381-386,  
687 <https://doi.org/10.1016/j.etp.2008.10.004>

688 Parrado, C., Mercado-Saenz, S., Perez-Davo, A., Gilaberte, Y., Gonzalez, S., Juarranz,  
689 A., 2019. Environmental Stressors on Skin Aging. Mechanistic Insights. *Front*  
690 *Pharmacol.* 10, 759. <https://doi.org/10.3389/fphar.2019.00759>

691 Persoz, C., Achard, S., Leleu, C., Momas, I., Seta, N., 2010. An *in vitro* model to  
692 evaluate the inflammatory response after gaseous formaldehyde exposure of lung  
693 epithelial cells. *Toxicol Lett.* 195, 99-105. <https://doi.org/10.1016/j.toxlet.2010.03.003>

694 Raaschou-Nielsen, O., Andersen, Z.J., Beelen, R., Samoli, E., Stafoggia, M.,  
695 Weinmayr, G., Hoffmann, B., Fischer, P., Nieuwenhuijsen, M.J., Brunekreef, B., Xun,  
696 W.W., Katsouyanni, K., Dimakopoulou, K., Sommar, J., Forsberg, B., Modig, L.,  
697 Oudin, A., Oftedal, B., Schwarze, P.E., Nafstad, P., De Faire, U., Pedersen, N.L.,  
698 Ostenson, C.G., Fratiglioni, L., Penell, J., Korek, M., Pershagen, G., Eriksen, K.T.,  
699 Sorensen, M., Tjonneland, A., Ellermann, T., Eeftens, M., Peeters, P.H., Meliefste, K.,  
700 Wang, M., Bueno-de-Mesquita, B., Key, T.J., de Hoogh, K., Concin, H., Nagel, G.,  
701 Vilier, A., Gioni, S., Krogh, V., Tsai, M.Y., Ricceri, F., Sacerdote, C., Galassi, C.,  
702 Migliore, E., Ranzi, A., Cesaroni, G., Badaloni, C., Forastiere, F., Tamayo, I., Amiano,  
703 P., Dorronsoro, M., Trichopoulou, A., Bamia, C., Vineis, P., Hoek, G., 2013. Air  
704 pollution and lung cancer incidence in 17 European cohorts: prospective analyses from  
705 the European Study of Cohorts for Air Pollution Effects (ESCAPE), *The Lancet*  
706 *Oncology*. 14, 813-822. [https://doi.org/10.1016/S1470-2045\(13\)70279-1](https://doi.org/10.1016/S1470-2045(13)70279-1)  
707 Ricquebourg, E., Achard, S., Bardet, G., Seta, N., Momas, I., 2015. Airway epithelium  
708 co-cultured with immune cells for a better assessment of the low dose effects of  
709 environmental pollutants on the inflammatory response. *Toxicol Lett*. 238, S132.  
710 <https://doi.org/10.1016/j.toxlet.2015.08.416>  
711 Rosdy, M., Clauss, L.C., 1990. Terminal epidermal differentiation of human  
712 keratinocytes grown in chemically defined medium on inert filter substrates at the air-  
713 liquid interface. *J Invest Dermatol*. 95, 409-414. [https://doi.org/10.1111/1523-](https://doi.org/10.1111/1523-1747.ep12555510)  
714 [1747.ep12555510](https://doi.org/10.1111/1523-1747.ep12555510)  
715 Rosdy, M., Pisani, A., Ortonne, J.P., 1993. Production of basement membrane  
716 components by a reconstructed epidermis cultured in the absence of serum and dermal

717 factors. Br J Dermatol. 129, 227-234. <https://doi.org/10.1111/j.1365->  
718 [2133.1993.tb11839.x](https://doi.org/10.1111/j.1365-2133.1993.tb11839.x)

719 Sato, J., Denda, M., Nakanishi, J., Koyama, J., 1998. Dry condition affects  
720 desquamation of stratum corneum *in vivo*. J Dermatol Sci. 18, 163-169.  
721 [https://doi.org/10.1016/s0923-1811\(98\)00037-1](https://doi.org/10.1016/s0923-1811(98)00037-1)

722 Schikowski, T., Hüls, A., 2020. Air Pollution and Skin Aging. Curr Environ Health  
723 Rep. 7, 58-64. <https://doi.org/10.1007/s40572-020-00262-9>

724 Singh, B., Maibach, H., 2013. Climate and skin function: an overview. Skin Res  
725 Technol. 19, 207-12. <https://doi.org/10.1111/srt.12043>

726 Verdin, A., Cazier, F., Fitoussi, R., Blanchet, N., Vié, K., Courcot, D., Momas, I., Seta,  
727 N., Achard, S., 2019. An *in vitro* model to evaluate the impact of environmental fine  
728 particles (PM<sub>0.3-2.5</sub>) on skin damage. Toxicol Lett. 305, 94-102.  
729 <https://doi.org/10.1016/j.toxlet.2019.01.016>

730 Warner, R.R., Stone, K.J., Boissy, Y., 2003. Hydration Disrupts Human Stratum  
731 Corneum Ultrastructure. J Invest Dermatol. 120, 275-284.  
732 <https://doi.org/10.1046/j.1523-1747.2003.12046.x>

733 Willers, M.S., Eriksson, C., Gidhagen, L., Nilsson, M.E., Pershagen, G., Bellander, T.,  
734 2013. Fine and coarse particulate air pollution in relation to respiratory health in  
735 Sweden, Eur Respir J. 42, 924-934. <https://doi.org/10.1183/09031936.0008821>

736 World Health Organization, Regional Office for Europe, 2010. WHO guidelines for  
737 indoor air quality: selected pollutants. World Health Organization. Regional Office for  
738 Europe. Accessed 20 July 2020. <https://apps.who.int/iris/handle/10665/260127>

739 World Health Organisation, 2018. Air pollution and health. Accessed 20 July 2020.  
740 <https://www.who.int/airpollution/en/>

741 **Tables**

742

743 **Table 1**

744 Summary of the main metallic and organic components of PMm (Cotonou, Benin -  
745 Cachon et al., 2014) and PMo (Dunkerque, France - Dergham et al., 2015).

---

<b>Chemicals</b>	<b>PMm</b> (ng/m <sup>3</sup> )	<b>PMo</b> (ng/m <sup>3</sup> )
Metallic elements (Al, Ba, Cr, Cu, Fe, Mn, Ni, Pb, Ti, V, Zn)	8,644	620
Water-soluble ions (Ca <sup>2+</sup> , Cl <sup>-</sup> , K <sup>+</sup> , Mg <sup>2+</sup> , Na <sup>+</sup> , NO <sub>3</sub> <sup>-</sup> , SO <sub>4</sub> <sup>2-</sup> )	6,225	2,437
Organic compounds (Benzene, Toluene, o,p-Xylene, Naphthalene...)	11	730

---

746

747 **Table 2**

748 Main elements of the qualitative profile of VOCs. Quantification was carried out using  
749 SPME fibers and GC/MS/FID analysis on the elements released on the third day of  
750 drying the paints. Concentrations determined as toluene equivalent from the FID signal.

---

<b>Chemicals</b>	<b>VOCwb (mg/m<sup>3</sup>)</b>	<b>VOCsb (mg/m<sup>3</sup>)</b>
Aromatic hydrocarbons (Toluene, Xylene, Ethylbenzene)	-	2,37
Aliphatic hydrocarbons (Decane, Nonane, Trimethyl cyclohexane...)	-	148.73
Substituted hydrocarbons (Propylene glycol, 2-butanone, Texanol...)	6.08	32.47

---

751

752 **Legends of the figures**

753 **Fig. 1.**

754 **Experimental design for the exposure of RHE to pollutants**

755 (A) Sequences of treatment for the exposure of RHE to pollutants. (B) Sequences of  
756 treatment event for the preconditioning of RHE by the semi-dry/humid airflow before  
757 exposure to pollutants. (C) Comparison of the different treatments and controls.

758

759 **Fig. 2.**

760 **Cellular functionality of RHE after exposure to pollutants.**

761 Results of MTT assays performed on RHE exposed to the different pollutants for 24h.  
762 n=3 independent experiments in duplicate, except for the negative control and SDS for  
763 which n=6 independent experiments with the MTT assay performed in duplicate for  
764 each. Conditions are compared to the negative control with \* p<0.05, \*\*\* p<0.001.

765

766 **Fig. 3.**

767 **Cellular functionality of RHE upon preconditioning by a semi-dry/humid airflow**  
768 **followed by exposure to pollutants.**

769 Results of MTT assays performed on RHE preconditioned or not (RH control) by a  
770 humid (90% RH) or a semi-dry (45% RH) airflow before being incubated with the  
771 different pollutants. n=2 independent experiments with the MTT assay performed in  
772 duplicate for each; \* p<0.05, \*\* p<0.01, \*\*\* p<0.001.

773

774 **Fig. 4.**

775 **Inflammatory response of RHE after exposure to pollutants.**

776 Profiling of cytokines/chemokines production in RHE exposed or not (negative control)  
777 to the different pollutants: (A) PM<sub>m</sub>, (B) PM<sub>o</sub>, and (C) VOCs and TS. n=1 experiment  
778 with the quantification performed in duplicate; \* p<0.05, \*\* p<0.01, \*\*\* p<0.001.

779

780 **Fig. 5.**

781 **Inflammatory response of RHE upon preconditioning by a semi-dry/humid airflow**  
782 **followed by exposure to pollutants.**

783 Quantification of (A) IL-1 $\alpha$ , (B) IL-8, and (C) RANTES in RHE preconditioned or not  
784 (RH control) by the humid (90% RH) or the semi-dry (45% RH) airflow before being  
785 incubated with the different pollutants. n=2 independent experiments with the  
786 quantification performed in duplicate; \* p<0.05, \*\* p<0.01, \*\*\* p<0.001.



Figure 1

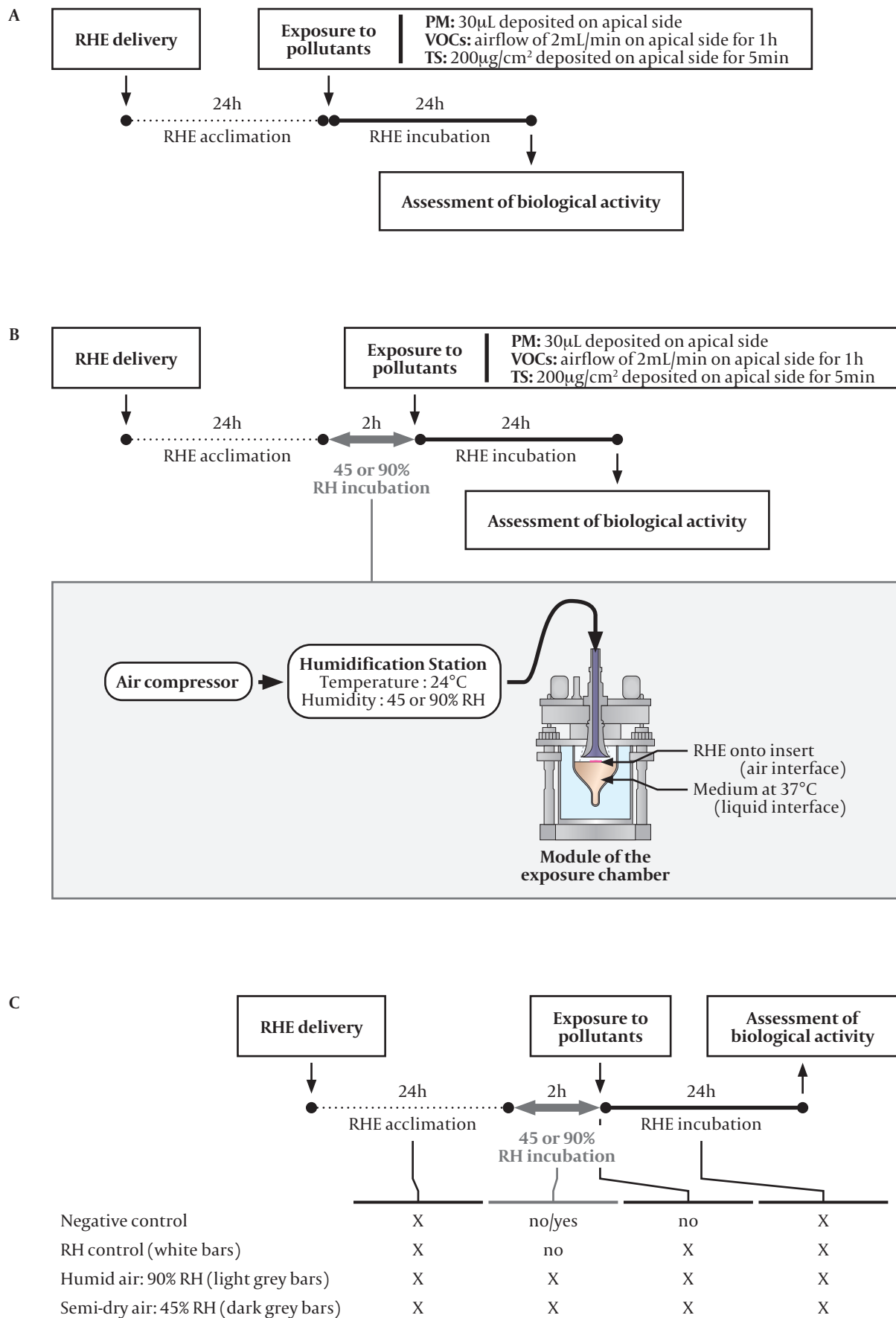


Figure 2

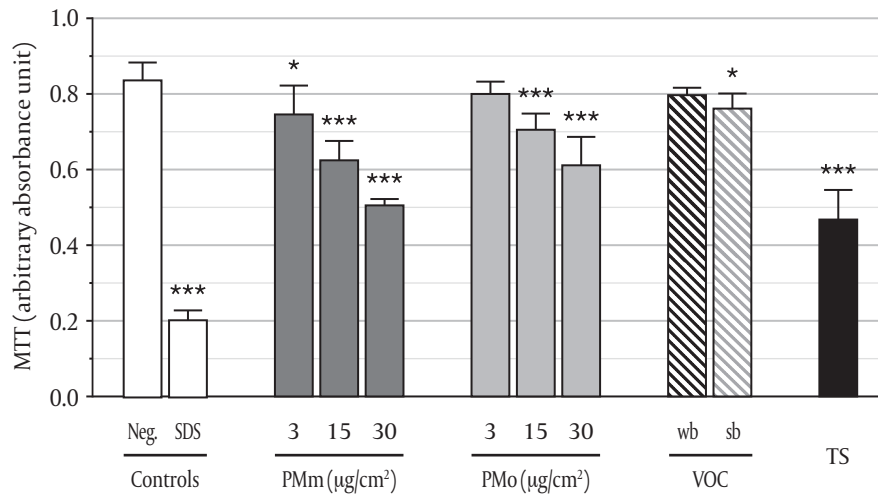
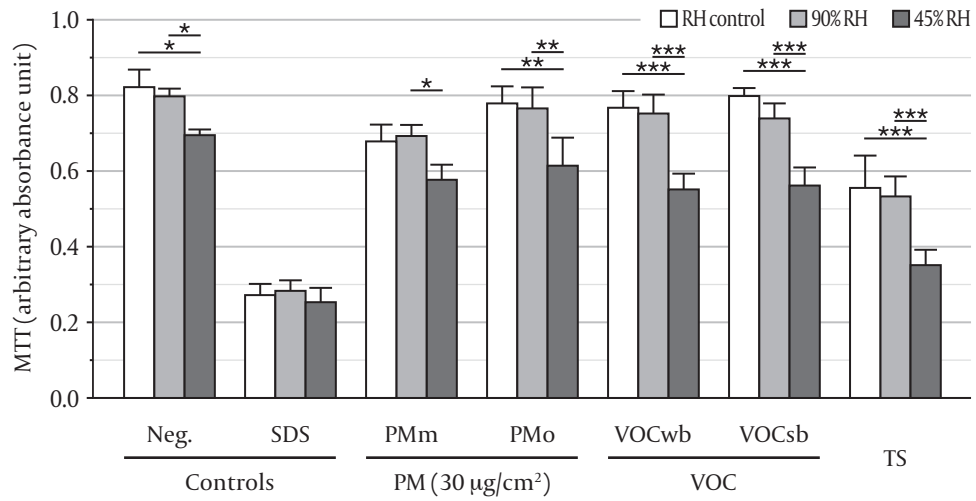


Figure 3



**Figure 4**

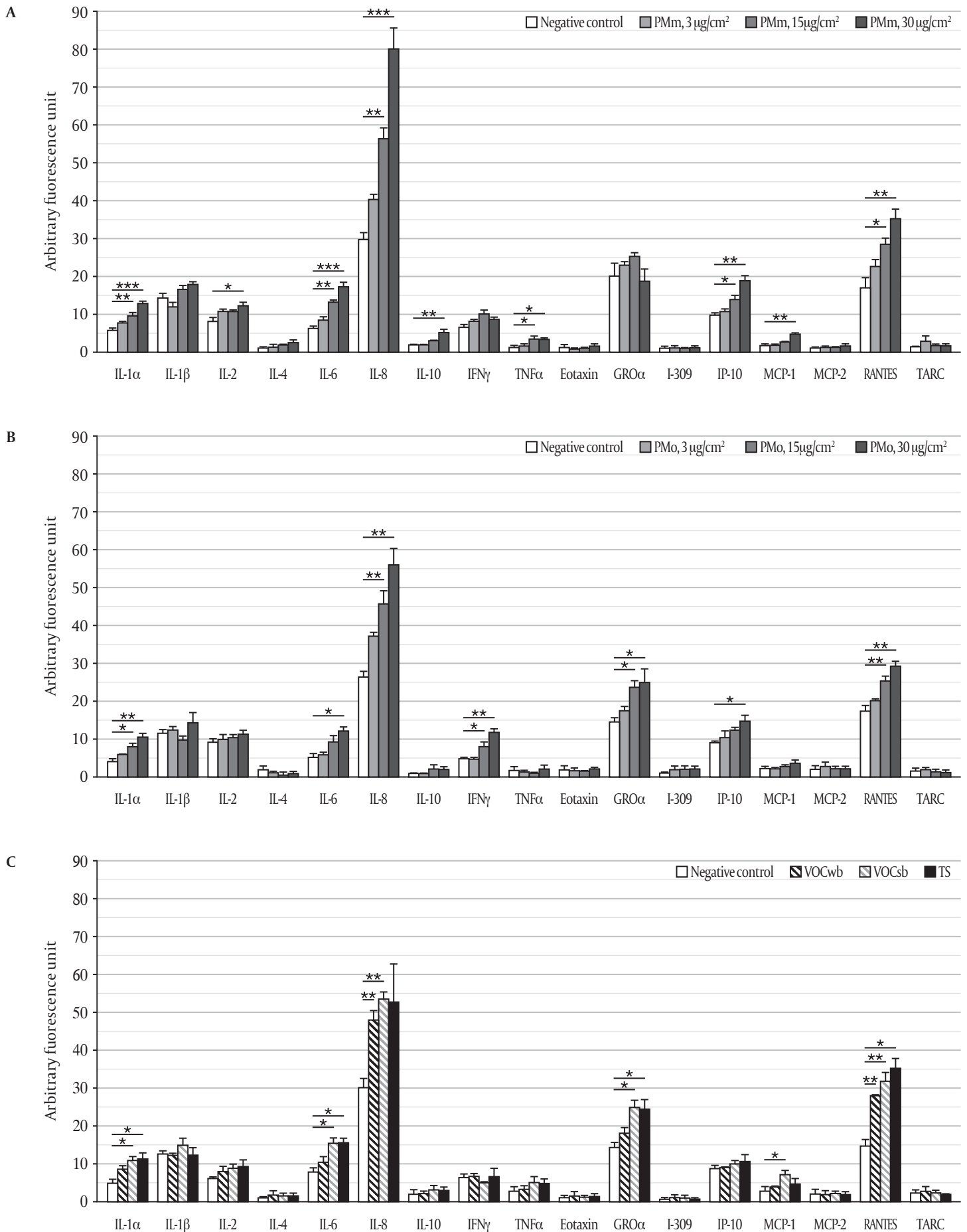
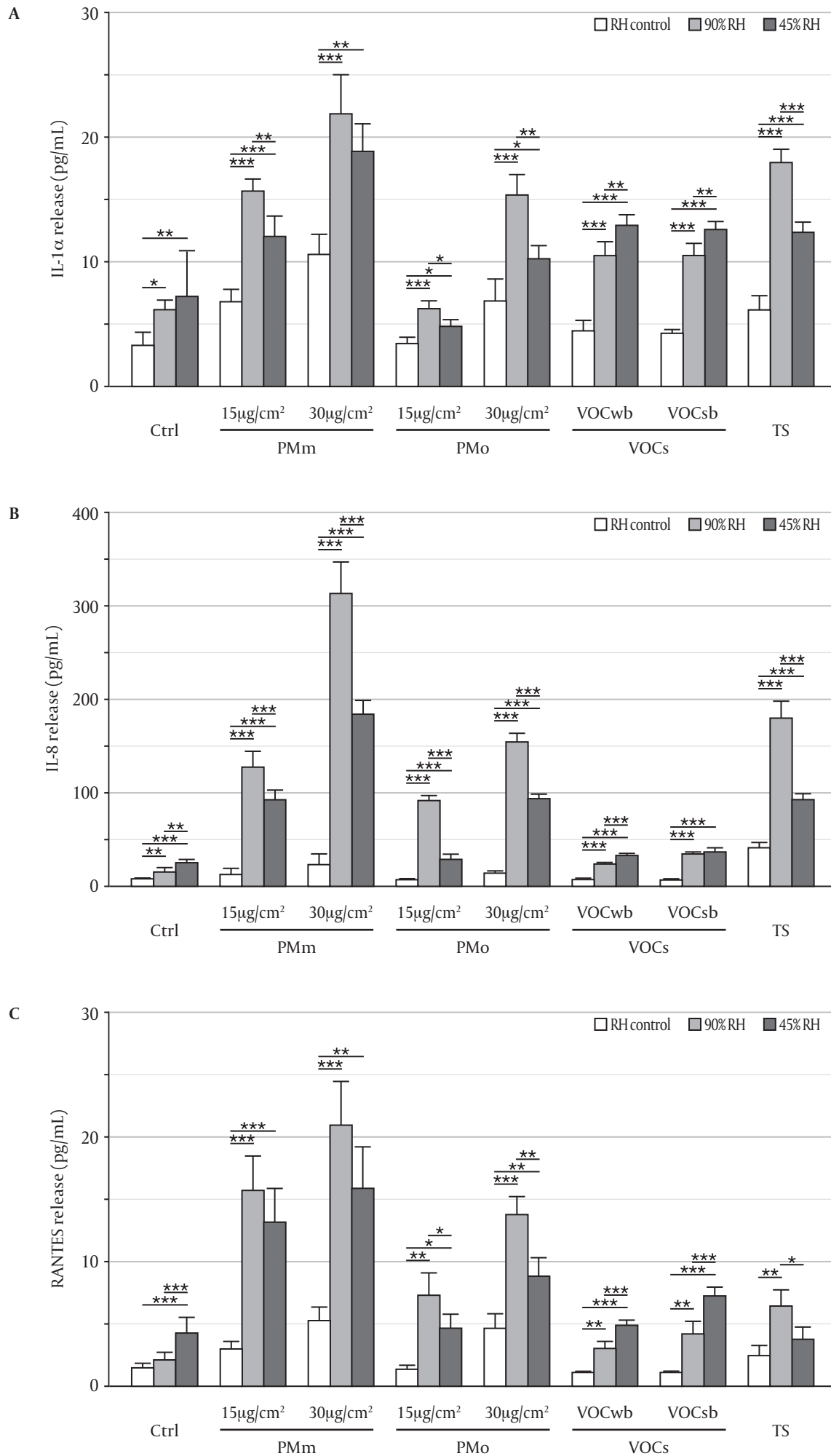
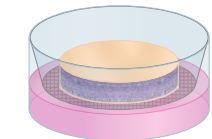


Figure 5

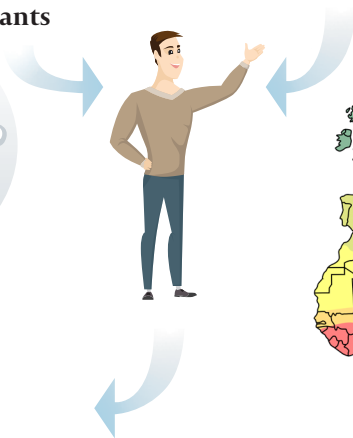




**Air pollutants**



***In vitro* skin model  
Inflammation**



**Air humidity**

